



## Normal coordinate analysis of the enol form of pentane-2,4-dione and its $^2\text{H}$ -isotopomers



CrossMark

Hamideh Fakheri,\* Sayyed Faramarz Tayyari,\* Mohammad Momen Heravi, Ali Morsali

Department of Chemistry, Mashhad Branch, Islamic Azad University, Mashhad and 9133736351, Iran

### Abstract

The harmonic and anharmonic vibrational frequencies of the cis-enol form of pentane-2,4-dione (PD) and its  $^2\text{H}$ -isotopomers were calculated by density functional theory method (DFT), performed at the B3LYP level. The results of the DFT calculations were subjected to a normal coordinate analysis, giving potential energy distribution (PED) and detailed assignments. Excellent agreement between observed and calculated anharmonic vibrational frequencies was obtained. It is well illustrated that the band frequencies resulted from movements of the enolic ring atoms are considerably coupled with the terminal groups' vibrations.

**Keywords:** Normal coordinate analysis; Density Functional Theory; pentane-2,4-dione; Vibrational spectra; Potential energy distribution (PED); Deuterated isotopomers; Acetylacetone

### 1. Introduction

Pentane-2,4-dione (PD), known as acetylacetone, is the simplest member of  $\beta$ -diketone compounds. PD has been the subject of a vast number of theoretical [1-11] and experimental [12-31] studies. Despite several spectroscopic studies on the vibrational spectra of PD [15-35], to the best of our knowledge, not only the quantitative analysis of vibrational spectra of this molecule has not been reported so far, but there are so many discrepancies between the vibrational band assignments of the titled molecule reported in the literature. Comparison of potential energy distribution (PED) of the vibrational normal modes of PD with those in its  $^2\text{H}$ -isotopomers demonstrates the effects of the weight of methylene and terminal groups on the chelated ring vibrational frequencies of the enol forms of  $\beta$ -diketones. It has been shown that the density functional theory (DFT) is a powerful tool for calculating the contributions of internal coordinates in the normal modes of vibrational movements (PED) in a molecule [36]. In the present work, based on the density functional theory, a normal coordinate analysis is performed for PD and its  $^2\text{H}$ -isotopomers ( $\text{d}_2\text{PD}$ ,  $\text{d}_6\text{PD}$ , and  $\text{d}_8\text{PD}$ ). The PED has also been calculated for the normal modes of vibrations to determine

quantitatively the contribution of each internal (or symmetry) coordinate in each vibrational normal mode. As it has been previously shown, this method gives more accurately the PED of vibrational frequencies than other conventional approaches [36].

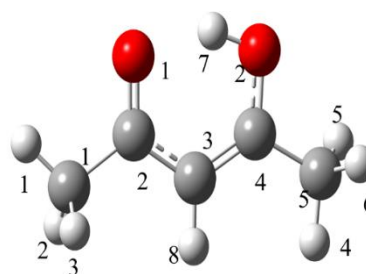


Fig. 1. Structure and atom numbering of PD.

### 2. Calculation methods

In the present study, all calculations for the cis-enol form of PD were performed by Gaussian-09 software [37]. The geometry optimization, harmonic vibrational frequencies, IR intensities, and Raman scattering

\*Corresponding authors e-mail: [hamidhfakheri@yahoo.com](mailto:hamidhfakheri@yahoo.com); ; [sftayyari@yahoo.com](mailto:sftayyari@yahoo.com).

Receive Date: 12 May 2020, Revise Date: 11 June 2020, Accept Date: 05 November 2020

DOI: 10.21608/EJCHEM.2020.30023.2645

©2021 National Information and Documentation Center (NIDOC)

calculations for the titled molecules were performed at the B3LYP [38,39] level using the 6-311++G(3df,2p) basis set. The anharmonic [40,41] vibrational frequencies were also calculated based on the optimized structure by using the B3LYP/6-311++G(P,d) level.

The calculated atomic displacements associated with the normal modes were illustrated by GaussView [42]. A normal coordinate analysis was carried out to provide a complete assignment of the fundamental vibrational wavenumbers for the cis-enol form of PD and its <sup>2</sup>H-isotopomers. By combining the displacement Cartesian coordinates of the atoms for each vibrational frequency and the Cartesian coordinates of atoms at the equilibrium position, obtained from Gaussian output, using the B3LYP/6-311++G(3df,2p) level, the displacement internal coordinates were calculated. The full sets of 49 standard internal coordinates containing 10 redundancies are defined as given in Table S1 (supplementary material). From these internal coordinates, a non-redundant set of the local symmetry coordinates was constructed by a suitable linear combination of internal coordinates (Table S1). Then all symmetry coordinates were normalized through all 39 normal coordinates, as described elsewhere [36,43,44]. The normalized symmetry coordinates

were used to calculate the potential energy distributions (PEDs) for each normal mode [36,43,44].

### 3. Results and discussion

The structure and atom numbering of the enol form of PD are given in Fig. 1. The calculated harmonic and anharmonic and the observed [18] vibrational band frequencies of PD along with the PED of the normal modes are depicted in Table 1. The corresponding values for deuterated derivatives of PD are listed in Tables S2-S4 (supplementary materials). As it is shown in these tables, there is excellent agreement between the observed and calculated anharmonic vibrational wavenumbers, except for OH/OD stretching vibrational wavenumbers. This deviation is not surprising if we remember that the potential function for the enolic proton motion in  $\beta$ -diketones is the symmetric double minimum type [2,45,46], which is not considered by Gaussian calculations. The most important theoretical and observed vibrational frequencies of PD and its deuterated derivatives are compared in Table 2 and are discussed in the following sections.

Table 1

Theoretical and experimental vibrational frequencies (cm<sup>-1</sup>) and PED of PD.<sup>a</sup>

sym	Theoretical					Experimental [18]			PED (%) <sup>b</sup>	
	F1	F <sub>an</sub>	F2	I <sub>IR</sub>	R <sub>A</sub>	IR(gas) I	R (liq.) I	I		
A'	3204	3055	3202	3	60		3096	5	vCH $\alpha$ (81)	
A'	3140	3005	3136	14	64	3017	10	3007	7	vaCH <sub>3</sub> (74), vsCH <sub>3</sub> (15)
A'	3135	2994	3132	10	50	3017		3007		vaCH <sub>3</sub> (73), vsCH <sub>3</sub> (15)
A''	3090	2948	3085	5	98	2976	6	2966	10	va'CH <sub>3</sub> (92)
A''	3088	2901	3083	7	61	2976		2966		va'CH <sub>3</sub> (91)
A'	3066	2540	3048	355	100	2800				vOH(71), vsCH <sub>3</sub> (21)
A'	3036	2924	3033	0	210	2941		2923	100	vsCH <sub>3</sub> (71), vaCH <sub>3</sub> (16), vOH(9)
A'	3030	2925	3029	11	201	2941		2923		vsCH <sub>3</sub> (69), vaCH <sub>3</sub> (17), vOH(11)
A'	1676	1641	1678	351	8	1642	19	1628	sh	vC=C(17), vC=O(17), $\delta$ CH $\alpha$ (10), $\delta$ OH(8), vC-CH <sub>3</sub> (8)
A'	1637	1612	1643	292	50	1624	77	1601	13	vC=C(11), vC=O(17), vC-C(7), $\delta$ OH(18), vC-CH <sub>3</sub> (9)
A'	1490	1445	1492	54	12	1464	10	1468	sh	$\delta$ aCH <sub>3</sub> (27), $\delta$ CH(16), vC-C(8), vC-O(8)
A''	1477	1407	1479	7	6			1401	1	$\delta$ a'CH <sub>3</sub> (72), $\pi$ CH <sub>3</sub> (17)
A''	1471	1434	1473	10	4	1427	17	1446	3	$\delta$ a'CH <sub>3</sub> (70), $\pi$ CH <sub>3</sub> (18)
A'	1470	1424	1472	6	8	1427		1426	8	$\delta$ aCH <sub>3</sub> (43), $\delta$ OH(11), $\delta$ CH(9)
A'	1456	1433	1460	141	2	1427				$\delta$ sCH <sub>3</sub> (14), $\delta$ aCH <sub>3</sub> (29), $\delta$ CH $\alpha$ (10), $\delta$ OH(8), vCC(7), vCO(7)
A'	1412	1376	1412	14	3			1370	8	$\delta$ sCH <sub>3</sub> (37), $\rho$ CH <sub>3</sub> (11), vC-CH <sub>3</sub> (10)
A'	1389	1350	1391	66	3	1365	10	1364	5	$\delta$ sCH <sub>3</sub> (48)

A'	1377	1315	1377	82	44	1302	47	1306	13	$\delta_s\text{CH}_3(20), \delta\text{OH}(14), \delta_a\text{CH}_3(11), \nu\text{C}=\text{C}(12), \nu\text{C}=\text{O}(10), \nu\text{CO}(9)$
A'	1268	1240	1268	145	6	1250	17	1247	13	$\nu\text{C}-\text{CH}_3(18), \nu\text{C}=\text{C}(12), \nu\text{C}-\text{C}(11), \delta_s\text{CH}_3(14), \delta\text{C}=\text{O}(9), \delta\text{OH}(8)$
A'	1191	1167	1195	16	7	1171	6	1169	7	$\delta\text{CH}_\alpha(23), \nu\text{C}=\text{O}(8), \delta_s\text{CH}_3(8), \nu\text{C}-\text{CH}_3(14), \delta\text{C}-\text{O}(8)$
A''	1059	1038	1062	1	2			1036	2	$\pi\text{CH}_3(42), \gamma\text{C}-\text{CH}_3(17), \delta_a'\text{CH}_3(14), \gamma\text{CH}_\alpha(8),$
A''	1043	1031	1045	8	0	1025	1			$\pi\text{CH}_3(37), \gamma\text{C}=\text{O}(16), \delta'\text{CH}_3(14), \text{gCH}(10)$
A'	1033	1012	1033	10	1	1005	sh	1000	4	$\rho\text{CH}_3(31), \delta_a\text{CH}_3(16)$
A'	1008	968	1009	14	9			993	4	$\rho\text{CH}_3(19), \nu\text{C}-\text{CH}_3(15), \delta_s\text{CD}_3(13), \nu\text{C}-\text{O}(10)$
A''	968	949	999	66	0	952	10			$\gamma\text{OH}(60), \gamma\text{C}=\text{O}(8)$
A'	942	930	943	2	4			930	7	$\delta\text{CCC}(13), \nu\text{C}-\text{C}(19), \rho\text{CH}_3(16), \nu\text{C}-\text{CH}_3(12)$
A'	917	866	917	37	2	913	9	915	2	$\nu\text{C}-\text{CH}_3(28), \nu\text{C}-\text{O}(11), \rho\text{CH}_3(11), \nu\text{C}=\text{C}(8)$
A''	790	773	794	32	1	768	40	785	5	$\gamma\text{CH}_\alpha(46), \pi\text{CH}_3(12), \gamma\text{C}-\text{CH}_3(12), \gamma\text{C}=\text{O}(10), \gamma\text{C}-\text{O}(19)$
A''	650	553	651	0	0					$\pi\text{CH}_3(26), \gamma\text{C}=\text{O}(28), \gamma\text{C}-\text{O}(22), \gamma\text{C}-\text{CH}_3(13)$
A'	642	700	647	13	12	636	9	641	35	$\nu\text{C}-\text{CH}_3(22), \delta\text{C}=\text{O}(18), \delta\text{C}-\text{O}(12), \delta\text{C}-\text{CH}_3(11)$
A''	553	564	559	0	2			554	15	$\gamma\text{C}-\text{CH}_3(38), \pi\text{CH}_3(24), \gamma\text{OH}(11), \gamma\text{C}-\text{O}(9), \gamma\text{C}=\text{O}(8)$
A'	510	508	512	11	3	508	20	508	4	$\delta\text{C}=\text{O}(15), \delta\text{C}-\text{O}(20), \delta\text{C}-\text{CH}_3(19), \rho\text{CH}_3(10)$
A'	397	382	397	3	0	397	s			$\delta\text{C}-\text{CH}_3(41), \rho\text{CH}_3(17)$
A'	369	362	372	7	4	362	s	369	5	$\delta\text{C}-\text{CH}_3(30), \delta\text{C}-\text{O}(17), \delta\text{CCC}(13), \rho\text{CH}_3(11)$
A'	229	224	231	3	0	210	w	227	7	$\delta\text{C}-\text{CH}_3(30), \delta\text{CCC}(19), \rho\text{CH}_3(10)$
A''	180	174	182	0	0					$\tau\text{CH}_3(20), \gamma\text{CH}_3(38), \gamma\text{C}-\text{O}(14)$
A''	148	142	148	0	0			140	sh	$\tau\text{CH}_3(50), \gamma\text{C}-\text{CH}_3(18), \gamma\text{C}=\text{O}(11), \gamma\text{C}-\text{O}(9)$
A''	118	115	119	1	0	120	w	104	w	$\gamma\text{C}-\text{CH}_3(35), \tau\text{CH}_3(30), \gamma\text{C}=\text{O}(12), \gamma\text{C}-\text{O}(11)$
A''	15	NC	21	0	0					$\tau\text{CH}_3(82)$

<sup>a</sup>  $F_1$  and  $F_{\text{an}}$  stand for harmonic and anharmonic vibrational wavenumbers obtained with the B3LYP/6-311++G\*\* level, respectively;  $F_2$  stands for harmonic wavenumbers calculated at the B3LYP/6-311++(3df,2p) level;  $I_{\text{IR}}$ , IR intensity (in km/mol);  $R_A$ , Raman activity (in  $\text{\AA}^4/\text{amu}$ );  $I$  stands for relative intensity;  $\nu$ ,  $\delta$ ,  $\gamma$ , and  $\tau$  stand for stretching, in-plane bending, out-of-plane bending, and torsion vibrations, respectively;  $\rho$  and  $\pi$  in-plane and out-of-plane rocking modes;  $\nu'$  and  $\delta'$  stands for out-of plane stretching and bending vibrations, respectively; NC, not converged. <sup>b</sup> The PEDs are only includes the contributions larger than 7%.

Table 2

Comparison of some important vibrational modes in PD and its 2H-isotopomers. a

Experimental [18]				Theoretical					
$d_0$	$d_2$	$d_6$	$d_8$	$d_0$	$d_2$	$d_6$	$d_8$		
3096		2300	3098	2303	3055		2279	3084	2303
2800		2027	2761	1970	2540		2000	2487	1912
1642		1633	1628	1614	1641		1640	1615	1598
1624		1544	1606	1524	1612		1536	1593	1497
1464		1448	1446	1371	1445		1442	1434	1359
1302		1082	1294	1078	1315		1094	1302	1078
1250		1273	1265	1274	1240		1270	1254	1271
952		707	952	691	949		706	952	718
362		360	337	335	362		356	335	330

<sup>a</sup> All values are in  $\text{cm}^{-1}$

### 3.1. OH/OD vibrations

It has been shown that the enol form of  $\beta$ -diketones exhibits an extremely broad band in the 3500–2200

$\text{cm}^{-1}$  region, which upon deuteration of the enolic proton appears as a new narrower band at the 2200–1800  $\text{cm}^{-1}$  region [46–51]. Upon increasing of hydrogen bond strength, the position of this band shifts towards lower frequencies, its bandwidth increases, and its intensity decreases. The low

intensity of this band is not surprising since its significant intensity is spread over a wide wavenumber region. Therefore, the estimation of the position of the band in the stronger intramolecular hydrogen bond of these compounds is not easily determined. However, the observed vibrational band frequencies of PD in the gas phase are reported to be occurring at about 2800  $\text{cm}^{-1}$  [18,27]. The corresponding band for  $\text{d}_6\text{PD}$  occurs at 2761  $\text{cm}^{-1}$  [18], about 40  $\text{cm}^{-1}$  lower than that of the light compound. The calculated anharmonic wavenumber for the OH stretching vibration in PD and  $\text{d}_6\text{PD}$  is 2540 and 2487  $\text{cm}^{-1}$ , respectively, which, its frequency shift is in agreement with the observed results. This frequency shift may be attributed to the effect of coupling between the OH stretching and  $\text{CH}_3/\text{CD}_3$  vibrational modes. Our PED calculations show that 21% of symmetric  $\text{CH}_3$  stretching contributes to this normal mode, which explains the frequency shifts upon deuteration. The OD stretching in the IR spectra of  $\text{d}_2\text{PD}$  and  $\text{d}_8\text{PD}$  appears at about 2027 and 1970  $\text{cm}^{-1}$ , respectively, which indicates that the OD stretching is also coupled with the  $\text{CH}_3/\text{CD}_3$  vibrations.

The broad IR band at 1302  $\text{cm}^{-1}$  is mainly OH bending, which is strongly coupled with asymmetric C-C=O and asymmetric C=C-O stretching and also weakly coupled to the symmetric  $\text{CH}_3$  deformation. The corresponding band in the IR spectrum of  $\text{d}_6\text{PD}$  occurs at 1294  $\text{cm}^{-1}$  [18]. In  $\text{d}_2\text{PD}$  and  $\text{d}_8\text{PD}$  this band disappears and a new band appears at 1082 and 1078  $\text{cm}^{-1}$ , respectively. The 1302  $\text{cm}^{-1}$  band was not considered by Ogoshi and Nakamoto [27] instead they assigned a shoulder at 1460  $\text{cm}^{-1}$  to the OH in-plane bending mode. The 1082  $\text{cm}^{-1}$  band in  $\text{d}_2\text{PD}$  is mainly OD in-plane bending vibration that is coupled with the C=C stretching and  $\text{CH}_3$  rocking mode, which is in agreement with the Matanović and Došlić assignment [23]. However, the 1082  $\text{cm}^{-1}$  band in the IR spectrum of  $\text{d}_2\text{PD}$  was solely assigned by Gutiérrez-Quintanilla *et al.* [34] and Ogoshi and Nakamoto [27] to the OD in-plane bending mode.

The broad band in about 950  $\text{cm}^{-1}$  in PD and  $\text{d}_6\text{PD}$ , which disappears in  $\text{d}_2\text{PD}$  and  $\text{d}_8\text{PD}$  is assigned to the OH out-of-plane bending slightly coupled to the C=O and C-O stretching vibrations. The corresponding band in  $\text{d}_2\text{PD}$  and  $\text{d}_8\text{PD}$  appears at 707 and 691  $\text{cm}^{-1}$ , respectively, which OD out-of-plane bending is coupled with the  $\text{CH}_3$  and  $\text{CD}_3$  out-of-plane rocking vibrations, respectively.

### 3.2. C=C, C-C, C=O, and C-O stretching vibrations

The two strong bands at 1642 and 1624  $\text{cm}^{-1}$  (Table 2), which could only be identified either by deconvolution [18] or using matrices [16,34,35], in the IR spectrum of gaseous PD are very close to those predicted by the calculated anharmonic wavenumbers

(1641 and 1612  $\text{cm}^{-1}$ , respectively) and are shown to be media sensitive. In the  $\text{H}_2$  matrix, these are observed at 1638 and 1618  $\text{cm}^{-1}$  [16] and in the liquid phase appear at 1625 and 1600  $\text{cm}^{-1}$  [18], respectively. According to our calculations, the former is assigned to the asymmetric C=C-C=O stretching vibrations (40%), which is somewhat coupled to the C-H $_{\alpha}$  and O-H in-plane bending and C- $\text{CH}_3$  stretching vibrations, and the latter is assigned to the symmetric C=C-C=O stretching (36%) strongly coupled to the OH in-plane bending (19%) and weakly coupled to the C- $\text{CH}_3$  stretching (9%). In  $\text{d}_6\text{PD}$  the corresponding bands appear at 1628 and 1606  $\text{cm}^{-1}$ , in  $\text{d}_2\text{PD}$  shift to 1633 and 1544  $\text{cm}^{-1}$ , and in  $\text{d}_8\text{PD}$  are observed at 1614 and 1524  $\text{cm}^{-1}$ , respectively [18]. These band frequency shifts are in agreement with our calculated results. By considering the corresponding bands in the gas phase IR spectra of  $\text{d}_2\text{PD}$ ,  $\text{d}_6\text{PD}$ , and  $\text{d}_8\text{PD}$  (see Table 2), it results that the deuteration of methyl groups causes a redshift for the higher and lower band frequencies of 14-19 and 18-20  $\text{cm}^{-1}$ , respectively, whereas, the deuteration of H $_{\alpha}$  and enol proton, shifts the higher and lower band frequencies of 9-14 and 80-82  $\text{cm}^{-1}$  towards lower frequencies, respectively, which confirms the results of our normal coordinate analysis. Ogoshi and Nakamoto [27] reported only a single band as the superposition of these two bands at 1623  $\text{cm}^{-1}$ , which solely assigned one of them to the C=O and the other to the C=C stretching vibrations. Gutiérrez-Quintanilla *et al.* [34] assigned the corresponding bands in  $\text{d}_2\text{PD}$  to the asymmetric and symmetric C=C+O stretching, respectively, which is almost in agreement with our results. Matanović and Došlić [23] assigned the 1642  $\text{cm}^{-1}$  to the asymmetric C=C-C=O stretching and OH in-plane bending, while the 1624  $\text{cm}^{-1}$  band was considered solely as C=O stretching and OH in-plane bending vibrations. Lozada-Garcia *et al.* [35] assigned the former to the C=O and asymmetric C=C-O stretching and OH in-plane bending vibrations. However, according to our calculations, the contribution of C-O stretching in this normal mode is not significant and the contribution of OH bending is considerably low (8%).

The 1464  $\text{cm}^{-1}$  band is assigned to the asymmetric C-C=C-O stretching vibrations, which is coupled to the  $\text{CH}_3$  deformation and  $\text{CH}_{\alpha}$  in-plane bending modes. The corresponding band in  $\text{d}_2\text{PD}$  and  $\text{d}_6\text{PD}$  appears at 1448 and 1446  $\text{cm}^{-1}$ , respectively, whilst in  $\text{d}_8\text{PD}$ , because of decoupling from both  $\text{CH}_3$  deformation and  $\text{CH}_{\alpha}$  bending, considerably shifts downward and appears at 1381  $\text{cm}^{-1}$ . This band was assigned by Ogoshi and Nakamoto [27] to the OH in-plane bending mode and assigned by Gutiérrez-Quintanilla *et al.* [34] and Matanović and Došlić [23] to the  $\text{CH}_3$  deformation, while Lozada-Garcia *et al.* [35] considered this band as  $\text{CH}_{\alpha}$  in-plane bending and asymmetric  $\text{CH}_3$  deformation.

The IR band at  $1250\text{ cm}^{-1}$  is also a complicated vibrational mode which includes C-CH<sub>3</sub>, C=C, C-C, and C-O stretching and CH<sub>3</sub> deformation and OH in-plane bending vibrations. Ogoshi and Nakamoto [27] considered this band solely as C-C stretching, while assigned by Lozada-Garcia *et al.* [35] to the symmetric C-C=C-C stretching and by Matanović and Došlić [23] assigned to the  $\nu_s\text{C}=\text{C}$  coupled with OH in-plane bending and C-CH<sub>3</sub> stretching, which is in agreement with our results, while ignored by Gutiérrez-Quintanilla *et al.* [34]. In d<sub>2</sub>PD, d<sub>6</sub>PD, and d<sub>8</sub>PD this band moves to 1273, 1265, and  $1271\text{ cm}^{-1}$ , respectively, which are also in agreement with our calculations.

### 3.3. CH<sub>3</sub>/CD<sub>3</sub> vibrations

Three bands at about 3017, 2970, and  $2940\text{ cm}^{-1}$  were observed in the IR spectrum of gaseous PD and d<sub>2</sub>PD [18] are attributed to the in-plane asymmetric, out-of-plane asymmetric, and symmetric CH<sub>3</sub> stretching vibrations, respectively, which is in agreement with the Lozada-Garcia *et al.* [35] and Matanović and Došlić [23] assignments. Ogoshi and Nakamoto [27] did not consider the CH<sub>3</sub> stretching vibrations.

The relatively broad IR band at  $1427\text{ cm}^{-1}$  seems to be the superposition of four bands, include mainly the degenerate CH<sub>3</sub> deformation vibrations,  $\delta\text{aCH}_3$ . In the H<sub>2</sub> matrix, four distinct bands are distinguished at 1462.6, 1431.7, 1427.3, and  $1424.2\text{ cm}^{-1}$  [35]. In the IR spectrum of d<sub>2</sub>PD, because of decoupling from OH and CH in-plane bending, the  $\delta\text{aCH}_3$  band shifts to  $1448\text{ cm}^{-1}$ . The corresponding bands in d<sub>6</sub>PD occur at about  $1050\text{ cm}^{-1}$ , whilst in d<sub>8</sub>PD appear at about  $1033\text{ cm}^{-1}$ .

The symmetric CH<sub>3</sub> deformations in PD and d<sub>2</sub>PD were observed at 1365 and  $1371\text{ cm}^{-1}$  [18], respectively. The IR spectra of the H<sub>2</sub> matrix of PD shows two distinct bands for symmetric CH<sub>3</sub> deformation at 1375.2 and  $1360.8\text{ cm}^{-1}$ , which are in agreement with the calculated anharmonic wavenumbers, 1376 and  $1350\text{ cm}^{-1}$ . The symmetric CD<sub>3</sub> deformations in the IR spectrum of PD appear at 1076 and  $1051\text{ cm}^{-1}$  [18], which are very close to the calculated anharmonic wavenumbers, 1082 and  $1055\text{ cm}^{-1}$ . In d<sub>8</sub>PD the higher frequency band is strongly coupled to the OD in-plane bending and appears at  $1112\text{ cm}^{-1}$  [18].

For PD, the Raman bands at 1036 and  $1000\text{ cm}^{-1}$  and IR bands at 1025 and  $1005\text{ cm}^{-1}$  are mainly caused by CH<sub>3</sub> rocking vibrations. The corresponding bands in d<sub>6</sub>PD were observed at 914, 904, 812,  $803\text{ cm}^{-1}$  and in d<sub>8</sub>PD occur at 902, 890, and  $802\text{ cm}^{-1}$  [18].

### 3.4. CH<sub>α</sub> vibrations

The weak Raman band at  $3096\text{ cm}^{-1}$  [18], which disappears upon deuteration, is assigned to the CH<sub>α</sub> stretching (81%). The corresponding band in the IR spectrum is very weak, so it is reported neither by Matanović and Došlić [23] nor by Lozada-Garcia *et al.* [35], while Ogoshi and Nakamoto [27] considered the  $2960\text{ cm}^{-1}$  band as CH<sub>α</sub> stretching vibration.

The weak IR band at  $1171\text{ cm}^{-1}$  is mainly resulted from CH<sub>α</sub> in-plane bending (23%), although it is highly coupled to other vibrational movements. Matanović and Došlić [23], Lozada-Garcia *et al.* [35] and Ogoshi and Nakamoto [27] also considered this band as  $\delta\text{CH}_\alpha$ . The corresponding band in d<sub>6</sub>PD is observed at  $1186\text{ cm}^{-1}$ . Upon deuteration of the proton at the α-position, this band disappears and a new band appears at about  $830\text{--}820\text{ cm}^{-1}$  [18] at the α-position, this band disappears and a new band appears at about  $830\text{--}820\text{ cm}^{-1}$  [18].

### 3.5. O...O stretching vibration

In the Far-IR spectra of PD and d<sub>2</sub>PD, the O...O stretching mode appears as a strong band at 362 and  $360\text{ cm}^{-1}$ , respectively, which is strongly coupled with the C-CH<sub>3</sub> bending and CH<sub>3</sub> rocking vibrations. The corresponding band in the Far-IR spectra of d<sub>6</sub>PD and d<sub>8</sub>PD is observed at 337 and  $335\text{ cm}^{-1}$ , respectively. Therefore, the O...O stretching vibration does not precisely reflect the hydrogen bond strength since it is considerably coupled to the terminal groups' vibrations.

## 4. Conclusions

The vibrational band frequencies of PD and its <sup>2</sup>H-isotopomers were assigned by using the calculated harmonic and anharmonic vibrational wavenumbers performed at the B3LYP level and normal coordinate analysis. Excellent agreement between experimental and calculated anharmonic wavenumbers obtained with the B3PLYP/6-311++G(p,d) level. A normal coordinate analysis, using the eigenvectors calculated at the B3PLYP/6-311++G(3df,2p), was performed for the titled molecules. The results of the normal coordinate analysis indicate that the vibrational modes related to the enolic ring atoms are highly coupled with the movements of terminal groups' atoms. The discrepancies between previously reported assignments were also discussed.

### 5. Conflicts of interest

There are no conflicts to declare.

### 6. Formatting of funding sources

This work was supported by the Islamic Azad University, Mashhad, 9133736351, Iran



- Sonnenberg, M. Hada, M. Ehara, K. Toyota, R. Fukuda, J. Hasegawa, M. Ishida, T. Nakajima, Y. Honda, O. Kitao, H. Nakai, T. Vreven, J. A. Montgomery, Jr., J. E. Peralta, F. Ogliaro, M. Bearpark, J. J. Heyd, E. Brothers, K. N. Kudin, V. N. Staroverov, T. Keith, R. Kobayashi, J. Normand, K. Raghavachari, A. Rendell, J. C. Burant, S. S. Iyengar, J. Tomasi, M. Cossi, N. Rega, J. M. Millam, M. Klene, J. E. Knox, J. B. Cross, V. Bakken, C. Adamo, J. Jaramillo, R. Gomperts, R. E. Stratmann, O. Yazyev, A. J. Austin, R. Cammi, C. Pomelli, J. W. Ochterski, R. L. Martin, K. Morokuma, V. G. Zakrzewski, G. A. Voth, P. Salvador, J. J. Dannenberg, S. Dapprich, A. D. Daniels, O. Farkas, J. B. Foresman, J. V. Ortiz, J. Cioslowski, and D. J. Fox, Gaussian, Inc., Wallingford CT, 2013.
- [38] A. D. Becke, *Phys. Rev. A* 38 (1988) 3098-3100. DOI:[10.1103/PhysRevA.38.3098](https://doi.org/10.1103/PhysRevA.38.3098)
- [39] A. D. Becke, *J. Chem. Phys.* 98 (1993) 5648-5652. DOI:[10.1063/1.464913](https://doi.org/10.1063/1.464913)
- [40] V. Barone, *J. Chem. Phys.* 122 (2005) 014108. DOI:[10.1063/1.1824881](https://doi.org/10.1063/1.1824881)
- [41] V. Barone, M. Biczysko, J. Bloino, *J. Phys. Chem. Chem. Phys.*, 16 (2014) 1759-1787. DOI:[10.1039/C3CP53413H](https://doi.org/10.1039/C3CP53413H)
- [42] GaussView, Version 6, R. Dennington, T. A. Keith, J. M. Millam, Semichem Inc., Shawnee Mission, KS, 2016.
- [43] F. Dolati, S. F. Tayyari, M. Vakili, *J. Mol. Struct.* 1094 (2015) 264-273. DOI:[10.1016/j.molstruc.2015.04.014](https://doi.org/10.1016/j.molstruc.2015.04.014)
- [44] S. F. Tayyari, M. Gholamhoseinpour, S. Emamian, E. R. Sammelson, *J. Fluor. Chem.* 184 (2016) 65-71. DOI:[10.1016/j.jfluchem.2016.02.013](https://doi.org/10.1016/j.jfluchem.2016.02.013)
- [45] S. F. Tayyari, M. Zahedi, F. Tayyari, F. Milani-Nejad, *J. Mo. Struct. Theochem*, 637 (2003) 171-181. DOI:[10.1016/S0166-1280\(03\)00533-5](https://doi.org/10.1016/S0166-1280(03)00533-5)
- [46] S. F. Tayyari, Z. Moosavi-Tekyeh, M. Zahedi-Tabrizi, H. Eshghi, *J. Mol. Struct.* 782 (2006) 191-199. DOI:[10.1016/j.molstruc.2005.08.012](https://doi.org/10.1016/j.molstruc.2005.08.012)
- [47] A. Nowroozi, S. F. Tayyari, H. Rahemi, *Spectrochim. Acta A* 59 (2003) 1757-1572. DOI:[10.1016/S1386-1425\(02\)00410-9](https://doi.org/10.1016/S1386-1425(02)00410-9)
- [48] S. F. Tayyari, R. Sammelson, F. Tayyari, H. Rahemi, *J. Mol. Struct.* 920 (2009) 301-309. DOI:[10.1016/j.molstruc.2008.11.020](https://doi.org/10.1016/j.molstruc.2008.11.020)
- [49] S. F. Tayyari, M. Vakili, A-R. Nekoei, H. Rahemi, Y. A. Wang, *Spectrochim. Acta A* 66 (2007) 626-636. DOI:[10.1016/j.saa.2006.04.002](https://doi.org/10.1016/j.saa.2006.04.002)
- [50] A-R. Nekoei, S. F. Tayyari, M. Vakili, S. Holakoei, A. H. Hamidian, R. E. Sammelson, *J. Mol. Struct.* 932 (2009) 112-122. DOI:[10.1016/j.molstruc.2009.05.045](https://doi.org/10.1016/j.molstruc.2009.05.045)
- [51] S. F. Tayyari, Z. Moosavi-Tekyeh, M. Soltanpour, A. R. Berenji, R. E. Sammelson, *J. Mol. Struct.* 892 (2008) 32-38. DOI:[10.1016/j.molstruc.2008.04.058](https://doi.org/10.1016/j.molstruc.2008.04.058)